



## Gelatine as a crustal analogue: Determining elastic properties for modelling magmatic intrusions

J.L. Kavanagh, Thierry Menand, Katherine A. Daniels

### ► To cite this version:

J.L. Kavanagh, Thierry Menand, Katherine A. Daniels. Gelatine as a crustal analogue: Determining elastic properties for modelling magmatic intrusions. *Tectonophysics*, 2013, 582, pp.101-111. 10.1016/j.tecto.2012.09.032 . hal-00811444

**HAL Id: hal-00811444**

**<https://hal.science/hal-00811444>**

Submitted on 10 Apr 2013

**HAL** is a multi-disciplinary open access archive for the deposit and dissemination of scientific research documents, whether they are published or not. The documents may come from teaching and research institutions in France or abroad, or from public or private research centers.

L'archive ouverte pluridisciplinaire **HAL**, est destinée au dépôt et à la diffusion de documents scientifiques de niveau recherche, publiés ou non, émanant des établissements d'enseignement et de recherche français ou étrangers, des laboratoires publics ou privés.

# Gelatine as a crustal analogue: Determining elastic properties for modelling magmatic intrusions

J.L. Kavanagh<sup>\*1</sup>, T. Menand<sup>2,3,4</sup>, K.A. Daniels<sup>5</sup>

<sup>1</sup>*School of Geosciences, Monash University, Clayton Campus, Clayton, VIC 3800,  
Australia*

<sup>2</sup>*Clermont Universit, Universit Blaise Pascal, Laboratoire Magmas et Volcans, BP  
10448, F-63000 Clermont-Ferrand, France*

<sup>3</sup>*CNRS, UMR 6524, LMV, F-63038 Clermont-Ferrand, France*

<sup>4</sup>*IRD, R 163, LMV, F-63038 Clermont-Ferrand, France*

<sup>5</sup>*School of Earth Sciences, University of Bristol, Bristol, BS8 1RJ, UK*

## Abstract

Gelatine has often been used as an analogue material to model the propagation of magma-filled fractures in the Earth's brittle and elastic crust. Despite this, there are few studies of the elastic properties of gelatine and how these evolve with time. This important information is required to ensure proper scaling of experiments using gelatine. Gelatine is a viscoelastic material, but at cool temperatures ( $T_r \sim 5\text{--}10^\circ\text{C}$ ) it is in the solid 'gel' state where the elastic behaviour dominates and the viscous component is negligible over short to moderate timescales. We present results from a series of experiments on up to 30-litres of maximum 30 wt% pigskin gelatine mixtures that document in detail how the elastic properties evolve with time, as a function of the volume used and gel concentration ( $C_{gel}$ ). Gelatine's fracture toughness is investigated by measuring the pressure required to propagate a pre-existing crack. In the gel-state, gelatine's Young's modulus can be calculated by measuring the deflection to the free-surface caused by an applied load. The load's geometry can effect the Young's modulus measurement; our results show its diameter needs to be  $\lesssim 10\%$  of both the container diameter and the gelatine thickness ( $H_{gel}$ ) for side-wall and base effects to be ignored. Gelatine's Young's modulus increases exponentially with time, reaching a plateau ( $E_\infty$ ) after several hours curing.  $E_\infty$  depends linearly on  $C_{gel}$ , while  $T_r$ ,  $H_{gel}$  and the gelatine's thermal diffusivity control the time required to reach this value. Gelatine's fracture toughness follows the same relationship as ideal elastic-brittle solids with a calculated surface energy  $\gamma_s = 1.0 \pm 0.2 \text{ J m}^{-2}$ . Scaling laws for gelatine as a crustal analogue intruded by magma (dykes or sills) show that mixtures of 2–5 wt% gelatine cured at  $\sim 5\text{--}10^\circ\text{C}$  ensure the experiments are geometrically, kinematically and dynamically scaled.

**Research Highlights**

- 2-5wt% gelatine mixtures at 5-10°C are good crustal analogues for dyke or sill experiments
- The Young's modulus gelatine solutions evolves with time to a plateau
- This Young's modulus plateau correlates linearly with gelatine concentration
- The time to plateau depends on the room temperature, gelatine thickness and its thermal diffusivity
- Gelatine's fracture toughness has a surface energy of  $\gamma_s = 1.0 \pm 0.1 \text{ Jm}^{-2}$

## Abstract

Gelatine has often been used as an analogue material to model the propagation of magma-filled fractures in the Earth's brittle and elastic crust. Despite this, there are few studies of the elastic properties of gelatine and how these evolve with time. This important information is required to ensure proper scaling of experiments using gelatine. Gelatine is a viscoelastic material, but at cool temperatures ( $T_r \sim 5\text{--}10^\circ\text{C}$ ) it is in the solid 'gel' state where the elastic behaviour dominates and the viscous component is negligible over short to moderate timescales. We present results from a series of experiments on up to 30-litres of maximum 30 wt% pigskin gelatine mixtures that document in detail how the elastic properties evolve with time, as a function of the volume used and gel concentration ( $C_{gel}$ ). Gelatine's fracture toughness is investigated by measuring the pressure required to propagate a pre-existing crack. In the gel-state, gelatine's Young's modulus can be calculated by measuring the deflection to the free-surface caused by an applied load. The load's geometry can effect the Young's modulus measurement; our results show its diameter needs to be  $\lesssim 10\%$  of both the container diameter and the gelatine thickness ( $H_{gel}$ ) for side-wall and base effects to be ignored. Gelatine's Young's modulus increases exponentially with time, reaching a plateau ( $E_\infty$ ) after several hours curing.  $E_\infty$  depends linearly on  $C_{gel}$ , while  $T_r$ ,  $H_{gel}$  and the gelatine's thermal diffusivity control the time required to reach this value. Gelatine's fracture toughness follows the same relationship as ideal elastic-brittle solids with a calculated surface energy  $\gamma_s = 1.0 \pm 0.2 \text{ J m}^{-2}$ . Scaling laws for gelatine as a crustal analogue intruded by magma (dykes or sills) show that mixtures of 2–5 wt% gelatine cured at  $\sim 5\text{--}10^\circ\text{C}$  ensure the experiments are geometrically, kinematically and dynamically scaled.

*Key words:* Gelatine, Dyke, Sill, Magma, Analogue Scaling

---

\* Corresponding author. Tel.: +61 3 9902 0062; fax:  
*Email address:* janine.kavanagh@monash.edu.

# 1 1 Introduction

2 Analogue experimentation is an important technique in science and engineer-  
 3 ing. In practice, it is the selection of appropriate analogue materials that is  
 4 often the biggest challenge in developing a set of experiments that are geomet-  
 5 rically, kinematically and dynamically scaled (*sensu* Hubbert (1937)). Exper-  
 6 iments that meet these criteria can be considered a laboratory-scale version  
 7 of the natural counterpart. In this paper we detail a series of experiments  
 8 carried out to document the properties of gelatine, a widely used analogue for  
 9 the Earth's crust.

10 Gelatine is an ideal analogue for those modelling homogeneous, isotropic and  
 11 elastic materials, for example it has been used by mechanical engineers (e.g. Crisp  
 12 (1952); Richards and Mark (1966)) and as a biological tissue analogue in the  
 13 medical sciences (e.g. Righetti et al. (2004)). The use of gelatine in geological  
 14 sciences has taken advantage of both its elastic and viscous properties, prov-  
 15 ing especially fruitful in developing our understanding magmatic intrusions  
 16 (dykes and sills) of volcanic feeder systems and their propagation dynamics  
 17 in the Earth's brittle and elastic crust (e.g. Fiske and Jackson (1972); Pol-  
 18 lard (1973); Pollard and Johnson (1973); Maaløe (1987); Hyndman and Alt  
 19 (1987); McGuire and Pullen (1989); Takada (1990); Heimpel and Olson (1994);  
 20 Takada (1994); McLeod and Tait (1999); Takada (1999); Dahm (2000); Muller  
 21 et al. (2001); Menand and Tait (2001); Ito and Martel (2002); Watanabe et al.  
 22 (2002); Menand and Tait (2002); Walter and Troll (2003); Acocella and Tibaldi  
 23 (2005); Rivalta et al. (2005); Cañón-Tapia and Merle (2006); Kavanagh et al.  
 24 (2006); Mathieu et al. (2008); Kervyn et al. (2009); Menand et al. (2010);  
 25 Maccaferri et al. (2010); Taisne and Tait (2011); Taisne et al. (2011)). The  
 26 photoelastic properties of gelatine have been of particular use to experimental

geologists (e.g. Taisne and Tait (2011)) and civil engineers (e.g. Farquharson and Hennes (1940); Crisp (1952); Tan (1947); Richards and Mark (1966)), where the internal stresses of a deformed gelatine can be visualised with the aid of polarised light. The prolific use of gelatine in the food industry has made a wealth of information available on its rheological properties (e.g. Watase and Nishinari (1980)). However, relatively few studies have documented the elastic properties of gelatine or how these evolve with time (e.g. Di Giuseppe et al. (2009))

We present results from a series of experiments that investigate the elastic properties of gelatine over a range of concentrations and volumes. Firstly the material properties of gelatine are detailed, followed by a description of the experimental setup and the theoretical basis for our measurements. The accuracy to which the experimentalist can determine the Young's modulus of the gelatine is evaluated by considering the uncertainties involved in the measurement, the effect of the properties of the applied load used to make the measurements and any apparatus side-wall or floor effects. In particular, our experimental results are focused on how the Young's modulus of the gelatine evolves with time. We also determined the gelatine's fracture toughness, a measure of the material's resistance to the growth of a crack. To aid the application of the results, we present some scaling laws that are appropriate for the use of gelatine as an analogue for the Earth's crust in geological studies focused on the formation controls and propagation dynamics of magma-filled fractures.

## 2 Material Properties

Gelatine is a polypeptide formed from the hydrolytic degradation of collagen (Ross-Murphy, 1992). It is classified as a 'physical gel' (e.g. Peyrelasse et al. (1996)), meaning that during gelification Van der Waals forces lead to the development of a complex and continuously connected three-dimensional network (lattice) of macromolecules (Djabourov et al., 1988a). The hydrogen bonds that are formed in this process are reversible and can be broken by changing temperature or pH (Djabourov et al., 1988b). From the onset, those working with gelatine have commented on its "fickle" nature (Richards and Mark, 1966). In order to use this material for quantitative modelling purposes, control needs to be kept on a range of factors including temperature, pH and gelatine concentration.

Gelatine is a viscoelastic material so during deformation it can display both elastic and viscous behaviour. High stresses applied for a short timescale cause the gelatine to behave elastically, whereas small stresses applied over a long time period will produce a viscous response. Viscoelasticity is traditionally modelled with an arrangement of springs and dashpots that can reproduce a measured creep curve (e.g. Richards and Mark (1966)). The proportion of elastic to viscous behaviour can be quantified by a phase shift  $\delta$  angle, also known as the "loss angle" (Mezger, 2002):

$$\delta = \arctan \frac{G''}{G'} \quad (1)$$

where  $G''$  is the energy loss (viscous-related) and  $G'$  is the energy stored (elastic-related) for a given strain or strain rate.  $\delta$  is equal to  $0^\circ$  for an ideal-elastic material and  $90^\circ$  for an ideal-viscous material. The transition from



viscously dominated to elastically dominated behaviour (or *vice versa*) occurs at the 'gel-point' (Djabourov et al., 1988b), which is the condition where elastic and viscous energies are equal ( $G'' = G'$ ,  $\delta = 45^\circ$ ). Gelatine is in the 'sol-state' (fluid) when  $G'' > G'$  and  $\delta > 45^\circ$ , but is in the 'gel-state' (solid) when  $G' > G''$  and  $\delta < 45^\circ$  (Ross-Murphy, 1992; Nelson and Dealy, 1993; Mezger, 2002). For gelatine, this marked change in mechanical properties can be brought about by changing the extent of deformation (strain) or temperature; the gel-point itself depends on time, temperature and concentration (Askeland et al., 2010; Di Giuseppe et al., 2009).

The focus of this paper will be on the ideal-elastic behaviour of gelatine. When a 2.5 wt% gelatine mixture at 10 °C is deformed at low strain it has  $G'$  two orders of magnitude higher than  $G''$  and  $\delta < 1^\circ$  (Di Giuseppe et al., 2009). At these conditions the material is in the 'gel-state' and it is possible to assume an almost ideal-elastic behaviour. When this is the case, Hooke's Law is obeyed and deformation is recoverable when high stresses are applied over short timescales: the applied stress ( $\sigma$ ) is proportional to strain ( $\gamma$ ) and independent of the strain rate ( $\dot{\gamma}$ ).

The elastic properties of a homogeneous and isotropic solid can be described fully by a combination of the Young's modulus  $E$  (ratio of tensile stress to tensile strain) and the Poisson's ratio  $\nu$  (the relative contractive to expansive response of the deformed material). For gelatine,  $\nu \simeq 0.5$  (e.g. Farquharson and Hennes (1940); Crisp (1952); Richards and Mark (1966); Righetti et al. (2004)) and is theoretically incompressible such that deformation results in no net volume change.

### 3 Experimental Set-up and Data Processing

#### 3.1 Young's Modulus Experiments

A series of twenty-six experiments were carried out to investigate the effect of time, gelatine concentration, volume, experimental apparatus dimensions and applied load properties on the calculated Young's modulus of solidified gelatine.

A gelatine solution was prepared by adding a measured quantity of approximately 80 °C deionised water to the required weight of gelatine granules (260 Bloom, 20 Mesh, Pigskin Gelatine supplied by Gelita UK) to achieve the desired concentration (see Table 1). The use of deionised water is required to produce a clear and transparent mixture which hinders bacterial growth, which would otherwise produce a cloudy appearance to the gelatine solid. This hot mixture was then poured into a specified container and any bubbles were removed from the surface using a spoon. To prohibit the formation of a toughened 'skin' on the gelatine surface by water evaporation, a thin layer of vegetable oil was poured on top. The container was then placed into a temperature-controlled cold room at 5–10 °C ( $T_r$ ), and the mixture temperature ( $T_0$ ) and time were recorded. The gelatine was left in the cold room for several hours until the mixture temperature had equilibrated with the surroundings.

One way of calculating the gelatine's Young's modulus is to measure the deflection imposed by a load applied to the gelatine's surface (Timoshenko and

Goodier, 1970):

$$E = \frac{M_L g (1 - \nu^2)}{D_L w}, \quad (2)$$

where  $D_L$  is the diameter (m) of the cylindrical load,  $M_L$  is its mass (kg),  $w$  is the displacement (m) caused, and  $g$  is the gravitational acceleration.

Measurement of the Young's modulus commenced once the gelatine was able to support a load placed on its free surface. The container was removed from the cold room to make the measurements and then replaced afterwards. All the oil was carefully removed from the surface of the gelatine prior to any measurement being taken, using a spoon and then paper towel in order to achieve complete contact between the load and the gelatine. The load was applied by carefully placing a rigid metallic cylinder of known mass and dimensions onto the gelatine surface (see Figure 1 for a schematic sketch of the experimental setup and Table 2 for experimental load properties). Using a digital micrometer attached to a fixed reference position, the displacement of the free surface was measured (with an estimated error of  $\pm 0.1$  mm) and recorded by hand. The load was applied just prior to the measurement being made, and the total time in which it was in contact with the gelatine was approximately 30 seconds per measurement.  $E$  was calculated systematically for the duration of each experiment; measurements were made using each of the loads when possible approximately every one to two hours for up to 140 hours after the gelatine was prepared (nearly six days). For each time interval, the gelatine was at ambient room temperature for an interlude of less than ten minutes before being returned to the cold room. No experimental load was applied to the gelatine surface between time steps. The displacement measurement ' $w$ ' and the properties of the load were input into equation 2) to calculate the

145 Young's modulus of the gelatine solid.

146 The experimental series considers gelatine concentration  $C_{gel}$  (2-30 wt%), tem-  
 147 perature of the cold room  $T_r$  (5-10 °C), volume of gelatine  $V_{gel}$  (0.5 to 30  
 148 litres), diameter of the experimental container  $D_C$  (8.6-40.0 cm), thickness of  
 149 the gelatine  $H_{gel}$  (4.1-27.0 cm), and applied load (with mass  $M_L$  of 25.5-2808.5  
 150 g and diameter  $D_L$  20.0-85.6 mm) (see Tables 1 and 2). These experiments  
 151 allowed the characterisation of the evolution of the Young's modulus of gela-  
 152 tine over a range of conditions and for the factors affecting our measurements  
 153 to be assessed.

### 154 3.2 Fracture Toughness Experiments

155 The fracture toughness  $K_c$  is a measure of a material's resistance to the growth  
 156 of a crack. The fracture toughness of gelatine solids was determined by ex-  
 157 perimental means, measuring the pressure required to propagate an existing  
 158 crack (following the analysis of Sneddon and Das (1971)). This experimen-  
 159 tal method for calculating the fracture toughness of gelatine solid is briefly  
 160 described by Menand and Tait (2002). However, the mathematical procedure  
 161 is not detailed explicitly. Therefore, here we present the experimental proce-  
 162 dure again and detail in the Appendix the mathematical method so that other  
 163 experimentalists can replicate this.

164 For these fracture-toughness experiments high-clarity pigskin-derived gelatine  
 165 (acid, 200 bloom) was supplied in granular form by SKW Bio-Systems. The  
 166 gelatine mixture was prepared by first hydrating 5 to 8 wt% gelatine powder  
 167 in distilled water, and then heating the solution to 60 °C until the powder was  
 168 completely dissolved. Sodium hypochlorite was then added to the solution so

that it contained 0.1 wt% of active chlorine, in order to prevent fungal and bacterial growth. This amount was kept small to minimise its potential effect on the gelatine mechanical properties.

The gelatine solution was poured into a cubic acrylic tank (30 cm wide) and left to solidify for 48 hours at room temperature. A thin layer of silicon oil was poured on the gelatine surface in order to avoid evaporation during solidification and prevent the development of a gradient in gelatine properties. The tank was only filled to two-thirds its height, immersing a metallic blade that was elliptical in cross-section and had been inserted 5 cm into the gelatine's base. The blade measured 20 cm in length with a 1 cm thickness at its base. Once the gelatine had solidified, the blade was carefully removed thus creating an empty edge-crack in the gelatine solid. Both the crack and the remaining part of the tank were then filled with water, and the tank was overturned so that in its final position the crack was oriented vertically and at the bottom of the gelatine solid (Figure 2a). An outlet enabled water to bleed off any excess pressure in the lower part of the tank, and so ensured the water pressure balanced precisely with the weight of the overlying gelatine. Thus there was no excess pressure within the crack. Moreover, the initial state of stress within the gelatine solid was hydrostatic. (The gelatine solid adheres to the tank walls and so there is no horizontal strain,  $\epsilon_x = \epsilon_y = 0$ . Using Hooke's law, the relationship between the three stress components is  $\sigma_x = \sigma_y = \frac{\nu}{(1-\nu)}\sigma_z$ ; and given that gelatine has a Poisson's ratio  $\nu = 0.5$ ,  $\sigma_x = \sigma_y = \sigma_z$ .)

These fracture toughness experiments were carried out at a room temperature of  $19 \pm 2^\circ\text{C}$ . At the beginning of an experiment, the Young's modulus of the gelatine was measured as described in Section 3.1 (using a load with diameter approximately one tenth of the tank width). The crack excess pressure was

then increased by injecting air using a thin capillary which protruded into the crack (Figure 2b). During this injection of air, any excess water bled off ensuring that only the crack buoyancy increased; the excess pressure in the other water-filled part of the tank remained nil. As more air entered the crack, its buoyancy increased until it was sufficient to fracture the gelatine at the tip of the crack (Figure 2c). The process was recorded by video camera, and from this video record the exact amount of air that was present within the crack just prior to the gelatine fracture was measured. The Young's modulus of the gelatine was systematically varied between experiments, by changing the concentration of gelatine used during preparation, and the amount of air needed to propagate the initial crack was recorded, as summarised in Table 3.

The fracturing of the gelatine solid was analysed within the Linear Elastic Fracture Mechanics framework, according to which a crack propagates once the stress intensity factor at its tip  $K_I$  exceeds the fracture toughness  $K_c$  of the solid host (Griffith, 1921). Measuring the height of air present in the crack enabled us to calculate the pressure distribution within the crack and thus the stress intensity factor at its tip following the method of Sneddon and Das (1971) (see Section 4.2 and Appendix). We thus measured the height of air just prior to the crack propagation, and equated the calculated stress intensity factor with the gelatine fracture toughness.

### 3.3 Data Processing

Data processing was undertaken in order to identify and quantify potential sources of uncertainty in the Young's modulus measurements before analysing the results. To account for experimental uncertainties, both the effect of the dimensions of the applied load relative to the size of the experimental con-

tainer and also the effect of the propagation of errors in the Young's modulus calculation have been considered. A data weighting procedure has then been carried out before modelling the experimental results.

### 3.3.1 Effect of Applied Load and Container Size

We calculate the Young's modulus of gelatine by measuring by how much its free surface is deformed by an applied load. In doing so, we effectively assume that the gelatine solid is semi-infinite. However, the finite lateral dimensions of the gelatine container and distance to its base may have an important effect by restricting the movement of the deformed gelatine.

Figure 3 shows the relationship between the calculated Young's modulus and the relative size of the applied load diameter and the experiment container ( $D_L/D_C$ ). Data from eight experiments at one time interval are shown (22 hours curing at 10 °C). These experiments have equal gelatine concentration (2.5 wt%), but a range of volumes (0.5–30 litres), measured by Loads 1–8 in ten container sizes (see Table 1). Pearson product-moment correlation coefficients ( $r$ ) were calculated for each experiment:

$$r = \frac{S_{xy}}{\sqrt{S_{xx}S_{yy}}}, \quad (3)$$

where

$$S_{xx} = \sum (x - \bar{x})^2 \quad S_{yy} = \sum (y - \bar{y})^2 \quad S_{xy} = \sum (x - \bar{x})(y - \bar{y}), (4)$$

and  $x$  and  $y$  are experimentally determined variables (in this case  $E$  and  $D_L/D_C$ ). The correlation coefficient ranges from -1 to +1;  $r=+1$  indicates a positive linear correlation,  $r=-1$  suggests a negative linear correlation, and

242  $r=0$  when no correlation is found. In the region  $D_L/D_C > 10\%$  the results  
 243 show a strong positive correlation ( $r \geq 0.65$ ), implying interaction between the  
 244 applied load and container walls is producing artificially high Young's modulus  
 245 calculations (an exception is experiment 3, where  $r=0.38$ ). However, when  
 246  $D_L/D_C < 10\%$  the correlation is poor and in this region the experimentalist can  
 247 be confident of avoiding sidewall effects. Providing this is the case, equation 2  
 248 holds and can be used to calculate the Young's modulus of the gelatine. Note  
 249 that from the experiments shown, only experiments with a larger volume (20–  
 250 30 litres) with Young's modulus measured with loads 3–8 fall into this category.

251 The Young's modulus measurements may also be affected by the distance to  
 252 the base of the experimental container. If we assume the gelatine is semi-  
 253 infinite and behaves as a purely elastic solid, we can estimate the stresses  
 254 variation with depth induced by a load applied to the surface. The largest  
 255 stress component induced by a load  $\sigma_0$  is the vertical component  $\sigma_z$ , which  
 256 can expressed as (Timoshenko and Goodier, 1970):

$$257 \quad \sigma_z = \sigma_0 \left[ 1 - \frac{8z^3}{(1 + 4z^2)^{3/2}} \right], \quad (5)$$

258 where  $z$  has been normalised by the diameter of the load  $D_L$ . Following this  
 259 expression, the stress induced by the load at a depth ten times its diameter is  
 260 only 0.4% of that imposed by the load at the surface.

261 We therefore recommend that both the lateral and vertical dimensions of the  
 262 container be at least ten times the diameter of the load to avoid both container  
 263 sidewall and base effects.



### 3.3.2 Propagation of Errors

The uncertainty associated with the Young's modulus (equation 2) was calculated according to the principles of the 'Propagation of Errors' (Bevington and Robinson, 2003), where the relative error is expressed as:

$$\frac{\Delta E}{E} = \sqrt{\left(\frac{\Delta M}{M}\right)^2 + \left(\frac{\Delta D_L}{D_L}\right)^2 + \left(\frac{\Delta w}{w}\right)^2}, \quad (6)$$

where:

$$w = \beta + X_1 - X_0. \quad (7)$$

$\beta$  is the thickness of the load,  $X_0$  is the distance to the unloaded surface and  $X_1$  is the distance to the surface of the applied load (both  $X_1$  and  $X_0$  are measured relative to a fixed point of reference). Values of  $M$ ,  $D_L$ ,  $\beta$ ,  $X_1$  and  $X_0$  used in the calculation are averages of three separate and successive measurements.  $\beta$ ,  $X_1$  and  $X_0$  have independent random errors such that calculated values of  $w$  have an absolute error ( $\Delta w$ ):

$$\Delta w = \sqrt{\Delta \beta^2 + \Delta X_1^2 + \Delta X_0^2}. \quad (8)$$

Following this, the 'compound uncertainty' associated with each measurement of  $w$  is calculated as  $\pm 0.3$  mm. As the Young's modulus of the gelatine increases with time, correspondingly the deflection caused by the applied load decreases. Therefore the magnitude of  $w$  relative to  $\Delta w$  increases with time, as does the compound uncertainty associated with  $E$  ( $\Delta E/E$ ). This is illustrated by the increasing size of the Young's modulus error-bars with time (Figure 4).

### 3.3.3 Weighting the data

At each time interval,  $E$  was calculated using the deflection caused by each individual load (an average of three successive measurements). So for example, the complete dataset from experiment 25 (4-litres of 2.5 wt% gelatine; Figure 5) comprised 14 time intervals at which the Young's modulus was measured by loads 3–8 (where possible). The Young's modulus calculations were thus based on a total of 294 measurements of  $X_0$  and  $X_1$ . In order that all the measurements for each experiment could be considered in the analysis, a data weighting process was carried out.

To account for the uncertainties associated with each Young's modulus measurement, the data were weighted ( $W$ ) taking into account both the precision of the measurement and also the applied load used to take the measurement. Table 4 shows the quantitative weightings (depending on the uncertainty in  $E$ ;  $W_{\Delta E}$ ) and qualitative weightings (depending on the applied load used;  $W_{\Delta Load}$ ).

Weighting the Young's modulus data was straightforward, with high precision data ( $\Delta E/E < 5\%$ ) being weighted most highly ( $W_{\Delta E} = 8$ ). In comparison, weighting the applied loads could only be done qualitatively. Loads 1, 2 and 8–11 had low weightings ( $W_{\Delta Load} = 1$  or 2) as these had the highest  $D_L/D_C$  values and so their data were most likely to suffer from container sidewall effects (see Figure 3). Loads 6 and 7 were also weighted poorly ( $W_{\Delta Load} = 2$  and 4, respectively), as their relatively high thicknesses causing stability issues). Load 5 exerted the lowest pressure and so inflicted only a small deflection to the gelatine surface; this deflection became increasingly small (and so measured with higher uncertainty) as the gelatine's Young's modulus increased during cooling. Therefore, Load 5 was weighted relatively low ( $W_{\Delta Load} = 4$ ).

Loads 3 and 4 were weighted most highly ( $W_{\Delta Load} = 8$ ), deemed to have the most favourable balance between causing a deflection of the gelatine surface that could be measured to high precision, whilst experiencing minimal interaction with the container sidewalls.

The sum of the weights ( $W_{\Delta E} + W_{\Delta Load}$ ) was used to give an overall weighting for each datum. This procedure enabled the 'best' data to have the strongest influence on the modelling results, whilst enabling all the data to be included in the analysis process.

## 4 Results

### 4.1 *Young's Modulus of Gelatine*

By measuring the deflection caused by a load applied to the surface of the solidified gelatine, we have been able to document the evolution of the gelatine's Young's modulus relative to a number of parameters. These will now be considered separately.

#### 4.1.1 *Effect of Time*

Figure 5 shows the Young's modulus evolution with time of a 4-litre 2.5 wt% concentrated gelatine mixture kept at 5 °C (Experiment 25). The results show that, over the range of experimental conditions reported here, the gelatine is not able to support an applied load until it has a Young's modulus of approximately 1000 Pa. The Young's modulus then evolves exponentially with time to reach a plateau maximum value after which, as long as the experimental conditions are unchanged, the Young's modulus can be considered approximately

constant with time. This exponential relationship between Young's modulus of the gelatine and time was documented for all the experiments:

$$E = E_{\infty}(1 - e^{-\frac{t}{\tau}}), \quad (9)$$

where  $E_{\infty}$  (the Young's modulus plateau; Pa) and  $\tau$  (hr) are both empirically based constants determined from the exponential fit, and  $t$  is time (hr). The values of  $E_{\infty}$  and  $\tau$  vary depending on  $V_{gel}$ ,  $T_r$  and  $C_{gel}$  (see Table 5). As it is not feasible to wait for  $E_{\infty}$  to be reached during the timescale of an experiment, we define  $0.9E_{\infty}$  as an "effective" Young's modulus plateau and  $t_{0.9E_{\infty}}$  as the time taken to reach within 10% of  $E_{\infty}$ . These values are provided as a guide for the experimentalist in Table 5. The only effects of decreasing the room temperature from 10 °C to 5 °C were to increase the rate of Young's modulus increase with time and so decrease  $t_{0.9E_{\infty}}$ .

The values of Young's modulus plateau reported on Table 5 were all measured with loads 3–8, so that in these experiments the height of gelatine was at least 2.7 times as large as the greatest load diameter. Therefore, according to equation (5), the stress at the base of the gelatine layer induced by the loads was less than 5% of their value, and the potential effect of the base of the tank on these values of Young's modulus plateau was neglected.

It should be noted that both the use of deionised water and the storing of the gelatine mixtures in a cold room (set at 5–10 °C) led to the inhibition of bacterial growth in the media. Thorough cleaning of the experimental container was also vital. Following these methods, our data shows that once the gelatine mixtures have reached their plateau in Young's modulus they can maintain this up to 140 hours after the initiation of the experiment.

#### 4.1.2 Effect of Concentration

For low concentrations ( $\geq 2$  wt% and  $< 5$  wt%), the Young's modulus plateau ( $E_{\infty}$ ) of gelatine is linearly correlated with the concentration of the mixture (with a Coefficient of Determination  $R^2 = 0.9992$ ), as shown in Figure 6 for equal  $V_{gel}$  and  $H_{gel}$  (Experiments 16, 25–28). Values of  $E_{\infty}$  were calculated according to models fit to weighted Young's modulus data for a range of applied loads (see Section 4.1.1). It is unclear whether or not this linear relationship can be extrapolated to more highly concentrated gelatine mixtures.

Highly concentrated mixtures of gelatine ( $\geq 5$  wt%) proved difficult to work with, both in terms of preparing the experiments and then measuring their Young's moduli during the gelification process. During preparation of the mixtures, difficulties were encountered dissolving such highly concentrated mixtures and also removing all bubbles from the highly viscous solution was unachievable so that creating a homogeneous solid was not possible. Once the mixtures were in the 'gel-state' additional problems arose when attempting to measure their Young's moduli. When the loads were applied to these very rigid solids they were insufficient to cause a deflection of the gelatine surface that could be measured precisely; even the heaviest applied loads (Loads 9–11, see Table 2) caused such small deflections that the calculated Young's modulus value would have very large errors.

Due to the problems associated with these experiments we present only average Young's moduli for each experiment (Experiments 29–33); these were averaged from measurements taken from the time when the gelatine was deemed to have reached its Young's modulus plateau, an assumption verified by the lack of correlation between Young's modulus and time (indicated by a low  $r$ ; see Table 6). The results suggest that more strongly concentrated gelatines have a higher

Young's modulus plateau strength, though the associated standard deviations of the data were so large we were unable to evaluate whether this relationship continues the linear trend identified in Figure 6.

The experimental setup and method described here to measure the Young's modulus of gelatine solids proved unsuitable for highly concentrated mixtures. In order to quantify the Young's modulus of highly concentrated gelatine mixtures ( $\geq 5$  wt% gelatine mixtures, where the Young's modulus  $\gtrsim 20,000$  Pa), equipment more often associated with measuring the strength of rocks would be required. These tests are however beyond the scope of this study.

#### 4.1.3 *Effect of Volume*

Volume appears to have no impact on the Young's modulus plateau ( $E_\infty$ ) of the gelatine mixtures, as experiments that used the same concentration of gelatine, stored at the same  $T_r$ , evolved to give the same value of  $E_\infty$  ( $\pm 500$  Pa; Figure 7). The small discrepancy between modelled values of  $E_\infty$  is assumed to be related to errors associated with the properties of the applied load and the measuring technique, as described above (Section 3.3.1). There is a broadly positive correlation between the volume of gelatine and the time taken to reach the plateau in Young's modulus (modelled from the weighted data), i.e. larger volumes of gelatine take longer to reach their Young's modulus plateau.

#### 4.1.4 *Effect of Layer Thickness*

The time to reach the Young's modulus plateau value appears to correlate well with the time needed for the gelatine to cool down to  $T_r$ , and so we can use this correlation to predict the time an experimentalist would have

to wait until the gelatine Young's modulus has reached its plateau value. The thermal diffusivity of gelatine is assumed to be that of its solvent, that is water:  $\kappa = 1.4 \cdot 10^6 \text{ m}^2 \text{ s}^{-1}$ . The different containers used in the Young's modulus experiments were made of PMP, PP or Perspex (PMMA), and the thermal diffusivity for these thermoplastic polymers is about  $10^{-7} \text{ m}^2 \text{ s}^{-1}$ , one order of magnitude lower than that of gelatine. Therefore, to a leading order, a gelatine solid cools down by conducting its heat through its upper surface, and the time  $t$  needed for thermal equilibrium is:

$$t = \frac{H_{gel}^2}{\kappa}, \quad (10)$$

where  $H_{gel}$  is the height of the gelatine solid in the container. Figure 8 compares this cooling time with the time  $t_{0.9E_\infty}$  taken to reach 90% of the Young's modulus plateau  $E_\infty$  for gelatine mixtures of various concentrations (2 wt% to 5 wt%), but all cured at the same temperature of 5 °C (Experiments 13–19 and 25–28, Table 1). We find reasonable agreement with a best linear fit:

$$t_{0.9E_\infty} \simeq (29.0 \pm 8.7) + (2.6 \pm 1.2) \frac{H_{gel}^2}{\kappa}. \quad (11)$$

Equation (11) gives experimentalists a first-order estimate of the time they would need to wait for before a 2 wt% to 5 wt% gelatine solid cured at 5 °C reaches its Young's modulus plateau.

#### 4.2 The fracture toughness of solidified gelatine

The stress intensity factor  $K_I$  at the tip of a two-dimensional, edge crack of height  $h$  can be expressed as:

$$K_I = \alpha \overline{\Delta P} \sqrt{\pi h}, \quad (12)$$

where  $\alpha$  is a dimensionless factor that accounts for the conditions at the solid boundary (Sneddon and Das, 1971; Lawn, 1993; Menand and Tait, 2002), and  $\overline{\Delta P}$  denotes the averaged excess pressure within the crack:

$$\overline{\Delta P} = \frac{1}{h} \int_0^h \Delta P(z) dz, \quad (13)$$

where  $z$  is the vertical distance with origin at the reservoir-gelatine interface (Figure 2a). Determining the value of  $\alpha$  is a mixed problem, which simplifies when the edge of the elastic solid is a free boundary (Sneddon and Das, 1971), as was the case in our experiments. We measured the value of the coefficient  $\alpha$  using the method of Sneddon and Das (1971), summarized in the Appendix.

Griffith (1921) and Irwin (1957) showed that the fracture toughness  $K_c$  of an ideal elastic and brittle solid is related to its Young's modulus  $E$  by the following theoretical relationship:

$$K_c = \sqrt{2\gamma_s E}, \quad (14)$$

where  $\gamma_s$  is the surface energy of the solid. This is the energy required to create a unit surface area within that solid, and is thought to depend only on the composition and temperature of the solid (Griffith, 1921).

The calculated values of gelatine fracture toughness are shown in Figure 9. Despite some scattering, we find that equation 14 fits reasonably well these values, and that our best fit is:

$$K_c = (1.4 \pm 0.1) \sqrt{E}. \quad (15)$$

This equation and Figure 9 show that provided the viscous behaviour of gelatine solids is negligible and deforms essentially elastically, gelatine solids be-



have as ideal elastic and brittle solids in that their fracture toughness  $K_c$  and their Youngs modulus  $E$  follow the theoretical relationship (equation 14) expected for such solids.

We find a best estimate for the gelatine surface energy:

$$\gamma_s = 1.0 \pm 0.2 \text{ J m}^{-2}. \quad (16)$$

Remarkably, this value is similar to the surface energy of brittle monocrystals such as diamond ( $\gamma_s = 6 \text{ J m}^{-2}$ ), silicon ( $\gamma_s = 1.2 \text{ J m}^{-2}$ ), silicon carbide ( $\gamma_s = 4 \text{ J m}^{-2}$ ), silica ( $\gamma_s = 1 \text{ J m}^{-2}$ ), sapphire ( $\gamma_s = 4 \text{ J m}^{-2}$ ), magnesium oxide ( $\gamma_s = 1.5 \text{ J m}^{-2}$ ), or lithium fluoride ( $\gamma_s = 0.3 \text{ J m}^{-2}$ ) (Lawn, 1993). We note, however, that in principle  $\gamma_s$  should depend on the composition and temperature of the solid (Griffith, 1921), and so the exact value of  $\gamma_s$  may vary from one type of gelatine to the other. But given the rather small range of values for brittle monocrystals, which are also similar to that for gelatine, we believe  $\gamma_s = 1.0 \pm 0.2 \text{ J m}^{-2}$  is a fair estimate for acid, pig-skin derived gelatine with Bloom values between 200 and 260. Experiments carried at lower temperatures than reported here will either result in higher Youngs moduli or take less time to reach their Youngs modulus plateau, but their fracture toughness will scale correspondingly following equation 15.

## 5 Geological Applications

Di Giuseppe et al. (2009) summarise the application of gelatine as an analogue material for studying tectonic scale processes. They concluded low concentration gelatine mixtures ( $\sim 2.5 \text{ wt\%}$ ) could be an appropriate analogue for upper crustal deformation experiments. Complementary to this, we now present scal-

ing laws appropriate for studying magmatic intrusion dynamics. The scaling for this case is distinct to that presented by Di Giuseppe et al. (2009) as the stress and strain relations are different, and in particular the strain rates for dyke propagation are many order of magnitude faster than those of tectonic processes.

### 5.1 *Scaling gelatine for experiments on dyke and sill propagation dynamics*

An ideal scaled experiment has an analogue material that obeys geometric, kinematic and dynamic similarity with its natural counterpart (Hubbert, 1937); only then can observations and results of the experiment be used to understand the behaviour of the natural system. Others workers have presented simple scalings for the use of gelatine in its elastic-state as a crustal analogue for studying the propagation dynamics of magma-filled fractures (Acocella and Tibaldi, 2005; Cañón-Tapia and Merle, 2006). We now expand on these to present a comprehensive guide for scaling gelatine for this type of geological experiment.

Unlike tectonic processes, which occur on a length scale comparable with the thickness of the crust, dyke propagation is characterised by a much smaller length scale. This characteristic length scale is the buoyancy length  $L_b$ , as defined by Taisne and Tait (2009), which is the length over which magma buoyancy driving ascent balances resistance from rock fracture:

$$L = L_b = \left( \frac{K_c}{\Delta \rho g} \right)^{\frac{2}{3}}, \quad (17)$$

where  $L_b$  is the length of the buoyant head region of the propagating dyke,  $K_c$  is the fracture toughness of the intruded medium and  $\Delta \rho$  is the density

difference between the intruding fluid and its surroundings. Dyke propagation is determined by a local buoyancy balance in the inflated head region of the dike, independent of the total buoyancy of the magma column between source and tip (Lister and Kerr, 1991; Taisne and Tait, 2009). In this case the reduced gravity ( $g'$ ) is the relevant parameter for scaling the dyke driving force:

$$g' = \frac{\Delta\rho}{\rho_{solid}}g. \quad (18)$$

The timescale for the experiments is obtained by combining  $L_b$  (equation 17) and  $g'$  (equation 18):

$$T = \sqrt{\frac{L_b}{g'}} = \rho_{solid}^{\frac{1}{2}} K_c^{\frac{1}{3}} (\Delta\rho g)^{-\frac{5}{6}}, \quad (19)$$

and from this the dyke velocity scale follows easily:

$$U = \frac{L_b}{T} = (\Delta\rho g)^{\frac{1}{6}} K_c^{\frac{1}{3}} \rho_{solid}^{-\frac{1}{2}}. \quad (20)$$

This approach provides the appropriate scales (length, time and velocity) for each experiment, as one varies one parameter or another, and so provides the appropriate scaling factors  $L^* = \frac{L_l}{L_n}$ ,  $T^* = \frac{T_l}{T_n}$  and  $U^* = \frac{U_l}{U_n}$ :

$$L^* = \left( \frac{K_c^*}{\Delta\rho^*} \right)^{\frac{2}{3}}, \quad (21)$$

$$T^* = \rho_{solid}^{*\frac{1}{2}} K_c^{*\frac{1}{3}} (\Delta\rho^*)^{-\frac{5}{6}}, \quad (22)$$

$$U^* = (\Delta\rho^*)^{\frac{1}{6}} K_c^{*\frac{1}{3}} \rho_{solid}^{*-\frac{1}{2}}, \quad (23)$$

where  $*$  refers to the ratio of the parameter values measured at the laboratory (subscript  $l$ ) and natural (subscript  $n$ ) scale.

Finally, the driving buoyancy pressure ( $P_b$ ) scale for dykes is:

$$P_b = \Delta\rho g L_b, \quad (24)$$

which leads to deformation of the host medium around the head of the dyke.

The elastic pressure scale ( $P_e$ ) associated with this deformation is:

$$P_e = \frac{E}{2(1-\nu^2)} \frac{\psi}{L_b}, \quad (25)$$

where  $E$  and  $\nu$  are the Young's modulus and Poisson's ratio of the elastic host, respectively, and  $\psi$  is the thickness (i.e. the opening) of the dyke head. These two stress scales balance each other during dyke propagation (e.g. Lister and Kerr (1991)), which gives:

$$E = 2(1-\nu^2)\Delta\rho g \frac{L_b^2}{\psi}. \quad (26)$$

The Poisson's ratio for gelatine solids is  $\nu \simeq 0.5$ , whereas that of rocks lies usually between 0.25 and 0.3. As a result, the factor  $2(1-\nu^2)$  varies by 15–20% between nature and laboratory experiments, and the Young's modulus scale factor simplifies as:

$$E^* = \Delta\rho^* L_b^* \left( \frac{L_b}{\psi} \right)^*. \quad (27)$$

Strictly speaking, field measurements made on the geometry of fossilised dykes inform only on the final static state once solidification has taken place, and not on the geometry of propagating dykes. The discrepancy between the propagating and the final static geometry will certainly be important for those dykes that reached the surface because their thickness will decrease as magma erupts at the surface and elastic deformation of surrounding rocks is released. However, because of mass balance the discrepancy should be marginal for

the majority of dykes, which stall in the crust and do not reach the surface; notwithstanding potential volume change due to solidification, the volume of a propagating dyke should be the same as the volume of a static dyke. This caveat aside, we can use the geometrical measurements made on solidified dykes as proxies for their geometry during propagation.

The aspect ratio  $\frac{\psi}{L_b}$  of solidified dykes in nature is typically of the order of  $10^{-4} - 10^{-3}$  (e.g. Gudmundsson (2011); Kavanagh and Sparks (2011)), and on the order of  $10^{-2} - 10^{-1}$  in gelatine experiments. Taking the following values as representative for natural dykes:  $K_c = 10^7 \text{ Pa m}^{\frac{1}{2}}$ ,  $\Delta\rho = 100 \text{ kg m}^{-3}$ ,  $\rho_{solid} = 2800 \text{ kg m}^{-3}$ , and for experimental conditions:  $K_c = 100 \text{ Pa m}^{\frac{1}{2}}$ ,  $\Delta\rho = 1000 \text{ kg m}^{-3}$  (air) or  $\Delta\rho = 10 \text{ kg m}^{-3}$  (water),  $\rho_{solid} = 1000 \text{ kg m}^{-3}$ , one gets:

$$L^* = 10^{-4}(\text{air}) \quad \text{or} \quad L^* = 2 \times 10^{-3}(\text{water}), \quad (28)$$

$$T^* = 2 \times 10^{-3}(\text{air}) \quad \text{or} \quad T^* = 9 \times 10^{-2}(\text{water}), \quad (29)$$

$$U^* = 5 \times 10^{-2}(\text{air}) \quad \text{or} \quad U^* = 2 \times 10^{-2}(\text{water}), \quad (30)$$

$$E^* = 10^{-6} - 10^{-5}(\text{air}) \quad \text{or} \quad E^* = 2 \times 10^{-6} - 2 \times 10^{-5}(\text{water}). \quad (31)$$

In the experiments,  $L_l \simeq 5 \text{ cm}$  with air or  $\simeq 1 \text{ m}$  with water; this corresponds in nature to  $L_n \simeq 500 \text{ m}$ , which seems reasonable. Likewise, a velocity of a couple of mm/s (water) or cm/s (air) in the experiments would give dyke velocities on the order of 0.1–0.5 m/s in nature, in good agreement with estimates of dykes velocities (White et al., 2011). As for elastic deformation, the Young's modulus of rocks typically lies in the range  $E_n = 10^9 - 10^{10} \text{ Pa}$ , and so properly scaled experiments should involve gelatine solids with Young's modulus in the range  $E_l = 10^3 - 10^5 \text{ Pa}$  when air is used as a magma analogue, or

$E_l = 2 \times 10^3 - 2 \times 10^5$  Pa when water is used instead. Both ranges include values that have typically been used in dyke and sill experiments, and the data presented in this paper shows that 2–5 wt% of gelatine is sufficient to reach this range of Young's modulus plateau (Figure 6).

These calculations suggest gelatine experiments for magmatic intrusion propagation (dykes or sills) carried out at  $\sim 5-10$  °C and with gelatine concentrations of 2–5 wt% are adequately scaled geometrically, kinematically and dynamically.

## 6 Conclusions

We present results from a series of experiments that quantify the evolution of the elastic properties of gelatine with time. At 5–10 °C gelatine is in the 'gel-state', over the range of stresses and strain rates presented here, and behaves like a solid, with almost ideal-elastic deformation. The Young's modulus of gelatine evolves with time, modelled best by an exponential relationship, with  $E$  evolving to a plateau value that would theoretically be achieved after an infinite amount of time. At low gelatine concentrations ( $< 5$  wt%) the plateau Young's modulus depends linearly on the concentration of gelatine, and different volumes of equally concentrated gelatine evolve to the same plateau value. The method we use to measure the Young's modulus of the gelatine requires that the diameter of the load is  $\lesssim 10\%$  the diameter of the experimental container and thickness of the gelatine solid in order for side-wall and base effects to be avoided; larger dimensions relative to the gelatine solid will affect and lead to artificially high calculated values. Fracture toughness measurements show the  $K_c$  of gelatine follows the same relationship as ideal elastic-brittle

solids: it is proportional to the square-root of the Young's modulus multiplied by twice its surface energy, which was calculated experimentally as  $1.0 \pm 0.2$  J m<sup>-2</sup>.

The transparent nature and photoelastic properties of gelatine mean deformations can be easily visualised and monitored, giving the experimental geologist insight into the propagation dynamics of magmatic intrusions. However, caution needs to be taken when using gelatine as an analogue for the Earth's elastic crust. These type of experiments are best carried out at 5–10 °C in order for the viscous component of gelatine's deformation behaviour to be negligible. At these temperatures gelatine is a good analogue for magmatic intrusion propagation in Earth's elastic crust; using gelatine concentrations from 2–5 wt% will ensure gelatine is adequately scaled geometrically, kinematically and dynamically.

## 7 Acknowledgements

JK gratefully acknowledges the support of a Monash University Margaret Clayton Women in Research Postdoctoral Fellowship, and a Leverhulme grant awarded to R.S.J. Sparks and J. Blundy at Bristol University's Geophysical Fluid Dynamics Laboratory where the Young's modulus experiments were carried out. The fracture toughness experiments were carried out at Institut de Physique du Globe de Paris in 1998 during TM's PhD, and the valuable help of Steve Tait and Gérard Bienfait is acknowledged. KAD acknowledges a NERC consortium grant. This is Laboratory of Excellence *ClerVolc* contribution n° 29. E. Di Giuseppe, M. Diez and N. Le Corvec are thanked for thought-provoking discussions that inspired this work. B. Taisne and an anonymous

reviewer are thanked for thoughtful comments which improved the manuscript.



## 8 Appendix

In the fracture toughness experiments, the pressure distribution ( $\Delta P$ ) within the crack just prior to its propagation was:

$$\Delta P(z) = (\rho_g - \rho_w)gz, \quad 0 \leq z \leq z_l, \quad (32)$$

$$\Delta P(z) = \rho_ggz - \rho_wgz_l, \quad z_l \leq z \leq h, \quad (33)$$

where  $z_l$  is the level of the air-water interface within the crack ( $z_l = 0$  when the crack is full of air),  $\rho_g$  and  $\rho_w$  are the density of the solid gelatine and water, respectively. The density of air  $\rho_a$  is assumed to be negligible. Following Sneddon and Das (1971), by expressing this crack excess pressure as  $\Delta P(z) = \overline{\Delta P}f(z)$ , the value of  $\alpha$  in equation (12) is then determined by calculating the value  $\Lambda(1)$ , where  $\Lambda$  is the solution of the following integral:

$$\Lambda(z) - \int_0^1 \Lambda(u)L(z,u)du = \frac{2}{\pi} \int_0^z \frac{f(s)ds}{\sqrt{z^2 - s^2}}, \quad 0 \leq z \leq 1, \quad (34)$$

where  $z$  has been normalised with respect to the crack height  $h$ ,  $u$  and  $s$  are integration variables, and:

$$L(z,u) = \frac{16zu}{\pi^2} \left[ \frac{z^2 + u^2}{(z^2 - u^2)^3} \ln \left( \frac{z}{u} \right) - \frac{1}{(z^2 - u^2)^2} \right], \quad \text{if } z \neq u, \quad (35)$$

and:

$$L(z,u) = \frac{4}{3\pi^2u}, \quad \text{if } z = u. \quad (36)$$

Equation (34) was solved using the gaussian quadrature method. This leads to  $n$  linear equations:

$$\Lambda(x_i) - \sum_{j=1}^n w_j L(x_i, x_j) \Lambda(x_j) = \frac{2}{\pi} \int_0^{x_i} \frac{f(s) ds}{\sqrt{x_i^2 - s^2}}, \quad (i = 1, 2, \dots, n), \quad (37)$$

to be solved in order to determine the values  $\Lambda(x_1), \Lambda(x_2), \dots, \Lambda(x_n)$ , using the values  $x_1, x_2, \dots, x_n$  and their respective weights  $w_1, w_2, \dots, w_n$  (as listed in Table 52.8 from Abramowitz and Stegun (1964)). The value of  $\alpha$  is then:

$$\alpha = \Lambda(1) = \frac{2}{\pi} \int_0^1 \frac{f(s) ds}{\sqrt{1^2 - s^2}} + \sum_{j=1}^n w_j L(1, x_j) \Lambda(x_j). \quad (38)$$

The gelatine fracture toughness  $K_c$  was then equated with the stress intensity factor (12), using the average excess pressure  $\overline{\Delta P}$  measured just prior to the crack propagation and the corresponding value of  $\alpha$  (equation 38).

## References

- Abramowitz, M., Stegun, I., 1964. Handbook of Mathematical Functions. Dover Publications Inc.
- Acocella, V., Tibaldi, A., 2005. Dike propagation driven by volcano collapse: A general model tested at Stromboli, Italy. *Geophysical Research Letters* 32 (8), L08308.
- Askeland, D., Fulay, P., Wright, W., 2010. The Science and Engineering of Materials, 6th Edition. Thomson Engineering.
- Bevington, P., Robinson, D., 2003. Data Reduction and Error Analysis for the Physical Sciences, 3rd Edition. Mc Graw-Hill, USA.
- Cañón-Tapia, E., Merle, O., 2006. Dyke nucleation and early growth from

- pressurized magma chambers: Insights from analogue models. *Journal of Volcanology and Geothermal Research* 158 (3-4), 207–220.
- Crisp, J., 1952. The Use of Gelatin Models in Structural Analysis. *Proceeding IB of the Institute of Mechanical Engineers* 12, 580–604.
- Dahm, T., 2000. On the shape and velocity of fluid-filled fractures in the earth. *Geophysical Journal International* 142 (1), 181–192.
- Di Giuseppe, E., Funiciello, F., Corbi, F., Ranalli, G., Mojoli, G., 2009. Gelatins as rock analogs: A systematic study of their rheological and physical properties. *Tectonophysics* 473 (3-4), 391–403.
- Djabourov, M., Leblond, J., Papon, P., 1988a. Gelation of aqueous gelatin solutions. i. structural investigation. *Journal de Physique France* 49 (2), 319–332.
- Djabourov, M., Leblond, J., Papon, P., 1988b. Gelation of aqueous gelatin solutions. II. Rheology of the sol-gel transition. *Journal de Physique France* 49, 333–343.
- Farquharson, F., Hennes, R., 1940. Gelatin models for photoelastic analysis of stress in earth masses. *Civil Engineering* 10 (4), 211–214.
- Fiske, R., Jackson, E., 1972. Orientation and growth of Hawaiian volcanic rifts: the effect of regional structure and gravitational stresses. *Proceedings of the Royal Society of London. Series A, Mathematical and Physical Sciences* 329, 299–326.
- Griffith, A., 1921. The phenomena of rupture and flow in solids. *Philosophical Transactions of the Royal Society of London, Series A: Mathematical and Physical Sciences* 221, 163–198.
- Gudmundsson, A., 2011. *Rock Fractures in Geological Processes*. Cambridge University Press.
- Heimpel, M., Olson, P., 1994. Buoyancy-driven fracture and magma transport

- through the lithosphere: models and experiments. *International Geophysics* 57, 223–240.
- Hubbert, M., 1937. Theory of scale models as applied to the study of geologic structures. *Bulletin of the Geological Society of America* 48 (10), 1459–1517.
- Hyndman, D., Alt, D., 1987. Radial dikes, laccoliths, and gelatin models. *Journal of Geology* 95, 763–774.
- Irwin, G., 1957. Analysis of stresses and strains near the end of a crack traversing a plate. *Journal of Applied Mechanics* 24, 361–364.
- Ito, G., Martel, S., 2002. Focusing of magma in the upper mantle through dike interaction. *J. geophys. Res* 107, doi:10.1029/2001JB000251.
- Kavanagh, J., Menand, T., Sparks, R., 2006. An experimental investigation of sill formation and propagation in layered elastic media. *Earth and Planetary Science Letters* 245 (3-4), 799–813.
- Kavanagh, J., Sparks, R., 2011. Insights of dyke emplacement mechanics from detailed 3d dyke thickness datasets. *Journal of the Geological Society* 168, 965–978.
- Kervyn, M., Ernst, G., de Vries, B., Mathieu, L., Jacobs, P., 2009. Volcano load control on dyke propagation and vent distribution: Insights from analogue modeling. *Journal of Geophysical Research* 114 (B3), B03401.
- Lawn, B., 1993. *Fracture of Brittle Solids*, 2nd Edition. Cambridge University Press, New York.
- Lister, J., Kerr, R., 1991. Fluid-mechanical models of crack propagation and their application to magma transport in dykes. *Journal of Geophysical Research-Solid Earth* 96 (B6), 10049–10077.
- Maaløe, S., 1987. The generation and shape of feeder dykes from mantle sources. *Contributions to Mineralogy and Petrology* 96 (1), 47–55.
- Maccaferri, F., Bonafede, M., Rivalta, E., 2010. A numerical model of dyke

- propagation in layered elastic media. *Geophysical Journal International* 180 (3), 1107–1123.
- Mathieu, L., van Wyk de Vries, B., Holohan, E., Troll, V., 2008. Dykes, cups, saucers and sills: Analogue experiments on magma intrusion into brittle rocks. *Earth and Planetary Science Letters* 271 (1-4), 1–13.
- McGuire, W., Pullen, A., 1989. Location and orientation of eruptive fissures and feeder dykes at Mount Etna; influence of gravitational and regional tectonic stress regimes. *Journal of Volcanology and Geothermal Research* 38 (3-4), 325–344.
- McLeod, P., Tait, S., 1999. The growth of dykes from magma chambers. *Journal of Volcanology and Geothermal Research* 92 (3-4), 231–245.
- Menand, T., Daniels, K., Benghiat, P., 2010. Dyke propagation and sill formation in a compressive tectonic environment. *Journal of Geophysical Research* 115 (B8), B08201.
- Menand, T., Tait, S., 2001. A phenomenological model for precursor volcanic eruptions. *Nature* 411, 678–680.
- Menand, T., Tait, S., 2002. The propagation of a buoyant liquid-filled fissure from a source under constant pressure: an experimental approach. *Journal of Geophysical Research* 107 (2306), 177–185.
- Mezger, T., 2002. *The Rheology Handbook*. Vincentz.
- Muller, J., Ito, G., Martel, S., 2001. Effects of volcano loading on dike propagation in an elastic half-space. *Journal of Geophysical Research-Solid Earth* 106 (B6), 11101–11113.
- Nelson, B., Dealy, J., 1993. Dynamic mechanical analysis using complex waveforms. Chapman & Hall, Cambridge, Ch. Dynamic mechanical analysis using complex waveforms.
- Peyrelasse, J., Lamarque, M., Habas, J., El-Bounia, N., 1996. Rheology of

- 729 gelatin solutions in the sol-gel transition. *Physical Review E* 53 (6), 6126–  
730 6133.
- 731 Pollard, D., 1973. Derivation and evaluation of a mechanical model for sheet  
732 intrusions. *Tectonophysics* 19 (3), 233–269.
- 733 Pollard, D., Johnson, A., 1973. Mechanics of growth of some laccolithic intru-  
734 sions in the Henry mountains, Utah, II: Bending and failure of overburden  
735 layers and sill formation. *Tectonophysics* 18 (3-4), 311–354.
- 736 Richards, R., Mark, R., 1966. Gelatin models for photoelastic analysis of grav-  
737 ity structures. *Experimental Mechanics* 6 (1), 30–38.
- 738 Righetti, R., Ophir, J., Srinivasan, S., Krouskop, T., 2004. The feasibility of  
739 using elastography for imaging the Poisson's ratio in porous media. *Ultra-  
740 sound in medicine & biology* 30 (2), 215–228.
- 741 Rivalta, E., Böttlinger, M., Dahm, T., 2005. Buoyancy-driven fracture ascent:  
742 Experiments in layered gelatine. *Journal of Volcanology and Geothermal  
743 Research* 144 (1-4), 273–285.
- 744 Ross-Murphy, S., 1992. Structure and rheology of gelatin gels: recent progress\*.  
745 *Polymer* 33 (12), 2622–2627.
- 746 Sneddon, I., Das, S., 1971. The stress intensity factor at the tip of an edge  
747 crack in an elastic half-plane. *International Journal of Engineering Science*  
748 9 (1), 25–36.
- 749 Taisne, B., Tait, S., 2009. Eruption versus intrusion? arrest of propagation  
750 of constant volume, buoyant, liquid-filled cracks in an elastic, brittle host.  
751 *Journal of Geophysical Research* 114 (B6), B06202.
- 752 Taisne, B., Tait, S., 2011. Effect of solidification on a propagating dike. *Journal  
753 of Geophysical Research* 116 (B1), B01206.
- 754 Taisne, B., Tait, S., Jaupart, C., 2011. Conditions for the arrest of a vertical  
755 propagating dyke. *Bulletin of Volcanology*, 1–14.

- 756 Takada, A., 1990. Experimental study on propagation of liquid-filled crack  
757 in gelatin: shape and velocity in hydrostatic stress condition. *Journal of*  
758 *Geophysical Research* 95, 8471–8481.
- 759 Takada, A., 1994. Accumulation of magma in space and time by crack inter-  
760 action. *International Geophysics* 57, 241–257.
- 761 Takada, A., 1999. Variations in magma supply and magma partitioning: the  
762 role of tectonic settings. *Journal of volcanology and geothermal research*  
763 93 (1-2), 93–110.
- 764 Tan, E., 1947. Stability of soil slopes. *Proceedings of the American Society of*  
765 *Civil Engineers* 73, 19–38.
- 766 Timoshenko, S., Goodier, J., 1970. *Theory of elasticity*. McGraw-Hill Higher  
767 Education.
- 768 Walter, T., Troll, V., 2003. Experiments on rift zone evolution in unstable  
769 volcanic edifices. *Journal of volcanology and geothermal research* 127 (1-2),  
770 107–120.
- 771 Watanabe, T., Masuyama, T., Nagaoka, K., Tahara, T., 2002. Analogue exper-  
772 iments on magma-filled cracks: competition between external stresses and  
773 internal pressure. *Earth Planets and Space* 54, 1247–1261.
- 774 Watase, M., Nishinari, K., 1980. Rheological properties of agarose-gelatin gels.  
775 *Rheologica Acta* 19 (2), 220–225.
- 776 White, R., Drew, J., Martens, H., Key, J., Soosalu, H., Jakobsdóttir, S., 2011.  
777 Dynamics of dyke intrusion in the mid-crust of iceland. *Earth and Planetary*  
778 *Science Letters* 304, 300–312.

Exp.	$C_{gel}$	$M_{gel}$	$V_{gel}$	$H_{gel}$	$D_C$	$T_r$ (°C)	$T_0$ (°C)
1	2.5	4	4	17.0	17.3	10	34.5
2	2.5	3	3	12.7	17.3	10	35.0
3	2.5	2	2	8.5	17.3	10	35.5
6	2.5	20	20	12.5	40.0*	10	36.0
7	2.5	30	30	18.8	40.0*	10	38.0
8	2.5	0.5	0.5	4.1	12.5	10	35.5
9	2.5	0.5	0.5	6.4	10.0	10	34.5
10	2.5	0.5	0.5	8.7	8.6	10	34.5
11	2.5	20	20	12.5	40.0*	5	34.0
12	2.5	30	30	18.8	40.0*	5	34.5
13	2	2	2	16.4	12.5	5	37.5
14	2	1	1	8.2	12.5	5	37.5
15	2	3	3	12.7	17.3	5	38.0
16	2	4	4	17.0	17.3	5	38.0
17	2	10	10	19.6	25.5	5	37.0
18	2	20	20	27.0	30.7	5	38.5
19	2	30	30	20.0	30.2*	5	44.5
25	2.5	4	4	17.0	17.3	5	40.5
26	3	4	4	17.0	17.3	5	39.5
27	3.5	4	4	17.0	17.3	5	39.0
28	4	4	4	17.0	17.3	5	38.0
29	5	4	4	17.0	17.3	5	35.0
30	5	4	4	17.0	17.3	5	64.0
31	10	4	4	17.0	17.3	5	60.0
32	20	4	4	17.0	17.3	5	65.0
33	30	4	4	17.0	17.3	5	56.0



Table 1: Table of experimental conditions.  $C_{gel}$  = gelatine concentration (wt%),  $M_{gel}$  = mass of tested gelatine plus water mixture (kg),  $V_{gel}$  = volume of tested gelatine plus water mixture (litres),  $H_{gel}$  = thickness of gelatine mixture ( $\pm 0.5$  cm),  $D_C$  = container diameter ( $\pm 0.1$  cm),  $T_r$  = cold room temperature,  $T_0$  = starting temperature of gelatine mixture ( $\pm 0.5$  °C). Experimental containers were circular in cross-section, except those indicated by \* which were square (measuring 40 cm x 40 cm) and † which were oblong (measuring 50 cm x 30 cm).  $H_{gel}$  was calculated retrospectively from the container surface area and tested volume.

	Material	$\beta$ (mm)	$M_L$ (g)	$D_L$ (mm)
Load <sub>1</sub>	Aluminium	27.9	393.8	81.6
Load <sub>2</sub>	Aluminium	18.0	255.0	81.6
Load <sub>3</sub>	Brass	12.2	50.6	25.1
Load <sub>4</sub>	Brass	9.2	37.9	25.1
Load <sub>5</sub>	Brass	6.2	25.5	25.0
Load <sub>6</sub>	Brass	11.3	35.9	22.6
Load <sub>7</sub>	Brass	14.3	37.8	20.0
Load <sub>8</sub>	Brass	8.9	48.5	30.0
Load <sub>9</sub>	Steel	23.9	130.2	30.0
Load <sub>10</sub>	Steel	92.8	2279.3	63.5
Load <sub>11</sub>	Steel	62.8	2808.5	85.6

Table 2: Properties of the experimental loads:  $\beta$  = thickness ( $\pm 0.1$  mm),  $M_L$  = mass of load ( $\pm 0.1$  g),  $D_L$  = diameter of load ( $\pm 0.1$  mm). In all cases the data are mean averages of three measurements. Loads are cylindrical.

Exp.	$\rho_g$ (kg m <sup>-3</sup> )	$\rho_w$ (kg m <sup>-3</sup> )	E (Pa)	$z_l$ (cm)	$\overline{\Delta P}$ (Pa)	$K_c$ (Pa m <sup>1/2</sup> )
123	1062.0	1000.0	1449 ± 14	2.25	89 ± 27	59 ± 18
124	1072.3	1000.0	3969 ± 100	1.25	156 ± 26	93 ± 15
125	1079.3	1000.0	7603 ± 125	1.00	176 ± 26	103 ± 15
126	1063.3	1000.0	1877 ± 36	3.10	54 ± 29	40 ± 21
127	1072.7	1001.0	3906 ± 161	3.15	65 ± 29	48 ± 21
128	1079.3	1000.6	7328 ± 116	0.00	270 ± 25	148 ± 14
129 <sup>‡</sup>	1025.5	1000.3	10959 ± 354	4.00	189 ± 27	175 ± 25
131	1015.6	999.4	2254 ± 57	2.20	85 ± 27	57 ± 18

Table 3: The values of gelatine fracture toughness  $K_c$  determined from eight successful experiments.  $z_l$  is the level of the air-water interface within the crack just prior to its propagation;  $z_l = 0$  when the crack is full of air.  $\overline{\Delta P}$  is the corresponding averaged excess pressure. The gelatine and water densities,  $\rho_g$  and  $\rho_w$ , were both measured to within 4 kg m<sup>-3</sup> and 1 kg m<sup>-3</sup>, respectively, and the air level  $z_l$  to within 2.5 mm.

<sup>‡</sup> The crack was initially 5.0 ± 0.2 cm high in all experiment, except in experiment 129 where it was 10 cm high.

Quantitative $W$	$\Delta E/E$ (%)	$W_{\Delta E}$
	<5	8
	5–10	7
	10–15	6
	15–20	5
	20–30	4
	30–50	3
	50–100	2
	>100	1
Qualitative $W$	<i>Applied Load</i>	$W_{\Delta Load}$
	Load <sub>1</sub>	1
	Load <sub>2</sub>	1
	Load <sub>3</sub>	8
	Load <sub>4</sub>	8
	Load <sub>5</sub>	4
	Load <sub>6</sub>	4
	Load <sub>7</sub>	2
	Load <sub>8</sub>	2
	Load <sub>9</sub>	1
	Load <sub>10</sub>	1
	Load <sub>11</sub>	1

Table 4: Weightings ( $W$ ) used to quantify the quality of Young's modulus measurement data. Quantitative-based weightings consider the uncertainty in  $\Delta E/E$ , whereas the effect of the load used to take the measurements could only be weighted qualitatively based on the results from Figure 2. The combined weightings ( $W_{\Delta E} + W_{\Delta Load}$ ) are then used in the subsequent data analysis.

Experiment	$C_{gel}$	$E_{\infty}$ (Pa)	$\tau$ (hr)	$0.9E_{\infty}$ (Pa)	$t_{0.9E_{\infty}}$ (hr)
13	2	4431±44	14	3988	34
14	2	4475 ±58	12	4028	28
15	2	4317 ±82	15	3885	35
16	2	4172±54	17	3755	38
17	2	3972±36	30	3575	70
18	2	3628±49	22	3265	52
19	2	4106±109	33	3695	75
25	2.5	7003±233	19	6303	44
26	3	10165±284	19	9149	44
27	3.5	12775±548	16	11498	37
28	4	15973±441	16	14376	39

Table 5: Model results showing  $E_{\infty}$  and  $\tau$  values (correct to the nearest hour) for an exponential best-fit model  $E = E_{\infty}(1 - e^{-\frac{t}{\tau}})$  of calculated gelatine Young's moduli against time for a select group of experiments with the same  $T_r$  (5 °C). As  $E_{\infty}$  can not be reached within the timescale of an experiment, we define  $0.9E_{\infty}$  as an "effective" Young's modulus plateau.  $t_{0.9E_{\infty}}$  is the time taken (correct to the nearest hour) to reach within 10% of  $E_{\infty}$ . See Table 1 for experiment settings.

Experiment	29	30	31	32	33
wt%	5	5	10	20	30
$\overline{E}$	$2.9 \times 10^4$	$3.6 \times 10^4$	$1.5 \times 10^5$	$7.1 \times 10^5$	$4.5 \times 10^5$
St. Dev.	$1.4 \times 10^4$	$2.0 \times 10^4$	$1.6 \times 10^4$	$1.4 \times 10^6$	$5.6 \times 10^5$
$r$	0.40	0.32	-0.11	0.10	-0.55
$n$	36	9	12	13	13

Table 6: Average Young's modulus of highly concentrated ( $\geq 5$  wt%) gelatine mixtures. An average of ' $n$ ' measurements of the Young's modulus is shown ( $\overline{E}$ , correct to 2 s.f.), measurements were taken periodically using a range of applied loads for several hours after 16.5 hours curing at 5 °C. Calculated standard deviations (St. Dev.) indicate a high degree of uncertainty. The low Pierson Product-Moment Correlation Coefficients ( $r$ ) suggests no correlation between the Young's modulus measurements and time, supporting the assumption that the measurements were all made when the Young's modulus had plateaued.

Figure 1. Schematic illustration of the Young's modulus measurement procedure on a gelatine solid able to support an applied load. The deflection caused by a load placed on the surface of the solidified gelatine is measured, and this information is combined with the properties of the load to calculate the Young's modulus of the material.

Figure 2. Three successive photographs taken during a fracture-toughness experiment. (a) An edge-crack is initially created at the base of a gelatine solid, and filled with water. The initial reservoir pressure matches exactly the weight of the overlying gelatine solid. (b) Air is injected through a capillary and within the crack. Any potential reservoir excess pressure is released, so that only the crack buoyancy increases during air injection (see text). (c) When the crack buoyancy is high enough, the air-filled crack fractures the gelatine and propagates vertically.

Figure 3. Young's modulus ( $E$ ) of 2.5 wt% gelatine solids, after approximately 22 hours curing at 10 °C, plotted against the diameter of the applied load relative to the diameter of the container ( $D_L/D_C$ ) for loads 1-8 (Table 2) and five container sizes (Table 1). In the region  $D_L/D_C > 10\%$  (unshaded) each experiment individually shows a positive correlation between  $E$  and  $D_L/D_C$  (see legend for Pearson product-moment correlation coefficients), indicating interaction between the load and container could produce artificially high calculated Young's moduli. Where  $D_L/D_C \lesssim 10\%$  (shaded) there appears to be no correlation between  $E$  and  $D_L/D_C$ , and here sidewall effects can be neglected. When no error bars can be seen, the error is smaller than the symbol size.

Figure 4. Young's modulus evolution with time of 4-litres of 3 wt% gelatine stored at 5 °C (Experiment 26). The Young's modulus was calculated from the deflection caused to the gelatine surface by Load 3 (see Table 2). Error bars show the uncertainty in  $E$  increases with time.

Figure 5. Young's modulus evolution with time of 4-litres of 2.5 wt% gelatine stored at 5 °C (Experiment 25). The Young's modulus was calculated from the deflection caused to the gelatine surface by a range of applied loads (loads 3-8; see Table 2). An exponential relationship best fits the data ( $E = E_\infty(1 - e^{-\frac{t}{\tau}})$ ), where  $E_\infty = 7003$  Pa and  $\tau = 19$  hr).  $E$  increases with time to an "effective plateau" ( $0.9E_\infty$ ) of 6300 Pa after 44 hours curing ( $t_{0.9E_\infty}$ ). The best-fit model (solid line) takes into account all measurements weighted according to  $\Delta E/E$  and the load used (see Table 4). The outliers at ~55 hours and ~98 hours are from Load 7; these data have low weighting on the fitted trend due to this load having high thickness and small diameter that caused stability issues.

Figure 6. Modelled plateau Young's modulus ( $E_\infty$ ) of a range of gelatine concentrations  $C_{gel}$  (Experiments 16, 25–28). Each test volume was 4-litres and was kept at 5 °C ( $T_r$ ) in an equivalent container. The best-fit model indicates there is a positive-linear correlation ( $R^2 = 0.9992$ ) between  $E_\infty$  and  $C_{gel}$ . More concentrated gelatine mixtures reach a higher Young's modulus plateau.

Figure 7. Relationship between the modelled Young's modulus plateau ( $E_\infty \pm \Delta E_\infty$ ) and gelatine mixture volume  $V_{gel}$  for 2 wt% gelatine mixtures cured at 5 °C (Experiments 13–19). The mean  $E_\infty$  (dashed line) is shown and is most closely modelled by the 4-litre experiment (Experiment 16). The Pearson product-moment correlation coefficient ( $r = 0.64$ ) indicates there is little or no correlation between  $E_\infty$  and  $V_{gel}$ . Gelatine mixtures of the same concentration ( $C_{gel}$ ) evolve to the same  $E_\infty \pm 500$  Pa independent of volume.

Figure 8. Comparison of the time  $t_{0.9E_\infty}$  needed to reach 90% of the Young's modulus plateau  $E_\infty$ , with the conductive cooling time  $H_{gel}^2/\kappa$  given by equation 10. Data points correspond to experiments 13 to 19 and 25 to 28 (Table 1). These experiments had gelatine concentrations between 2wt% and 5wt%, and were all cured at 5 °C. The plateau time appears to correlate linearly with the cooling time: the curve is the best linear fit,  $t_{0.9E_\infty} \simeq (29.0 \pm 8.7) + (2.6 \pm 1.2) \frac{H_{gel}^2}{\kappa}$  (equation 11,  $R^2 = 0.3211$ ); 95% confidence limits are indicated by dashed lines.

Figure 9. The fracture toughness  $K_c$  of gelatine solids as a function of their Young's modulus  $E$ . The curve is the best fit through the data:  $K_c = (1.4 \pm 0.1) \sqrt{E}$  (equation 18,  $R^2 = 0.8196$ ), with the 95% confidence limits (dashed lines).



Figure 1

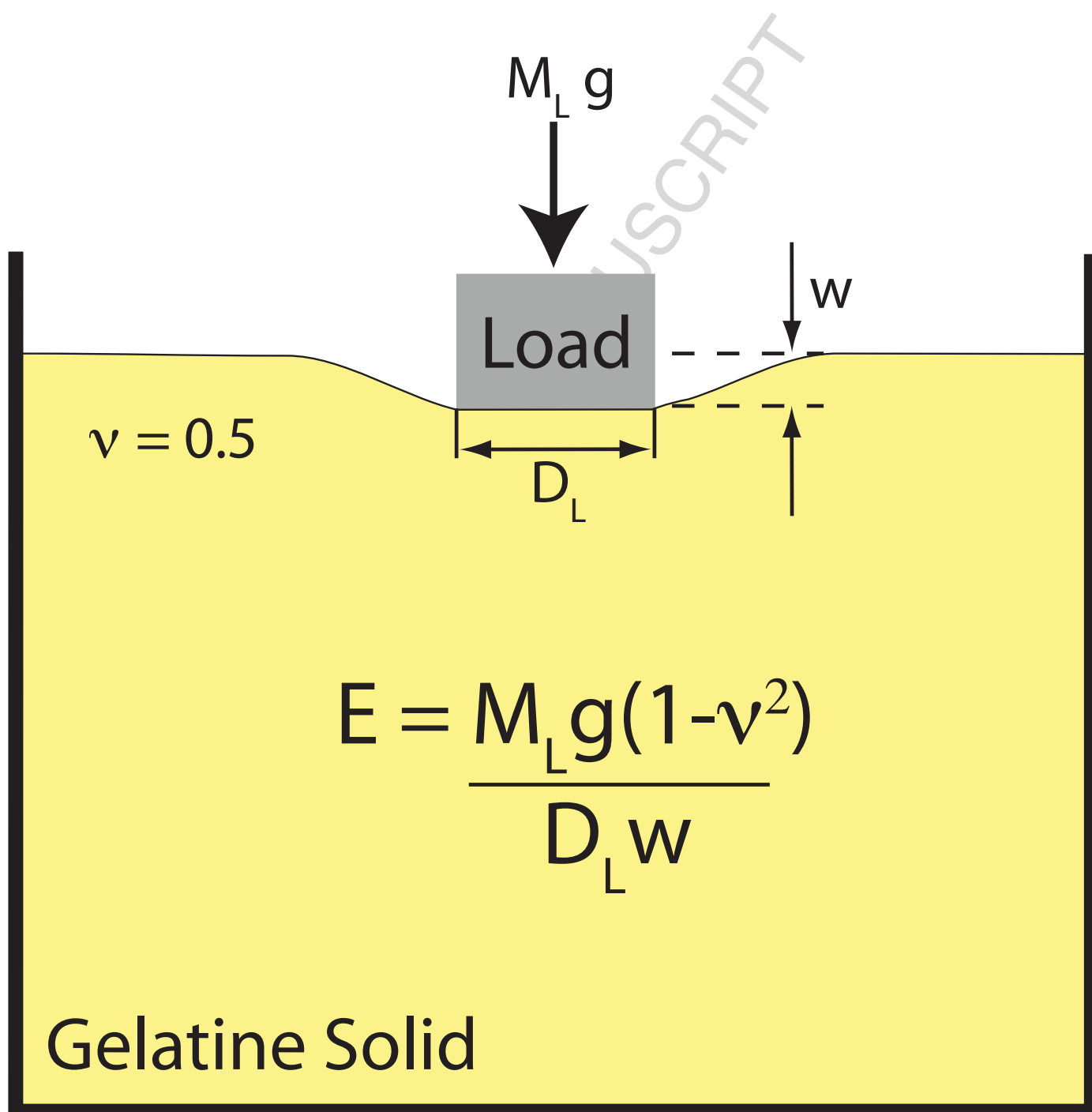


Figure 2

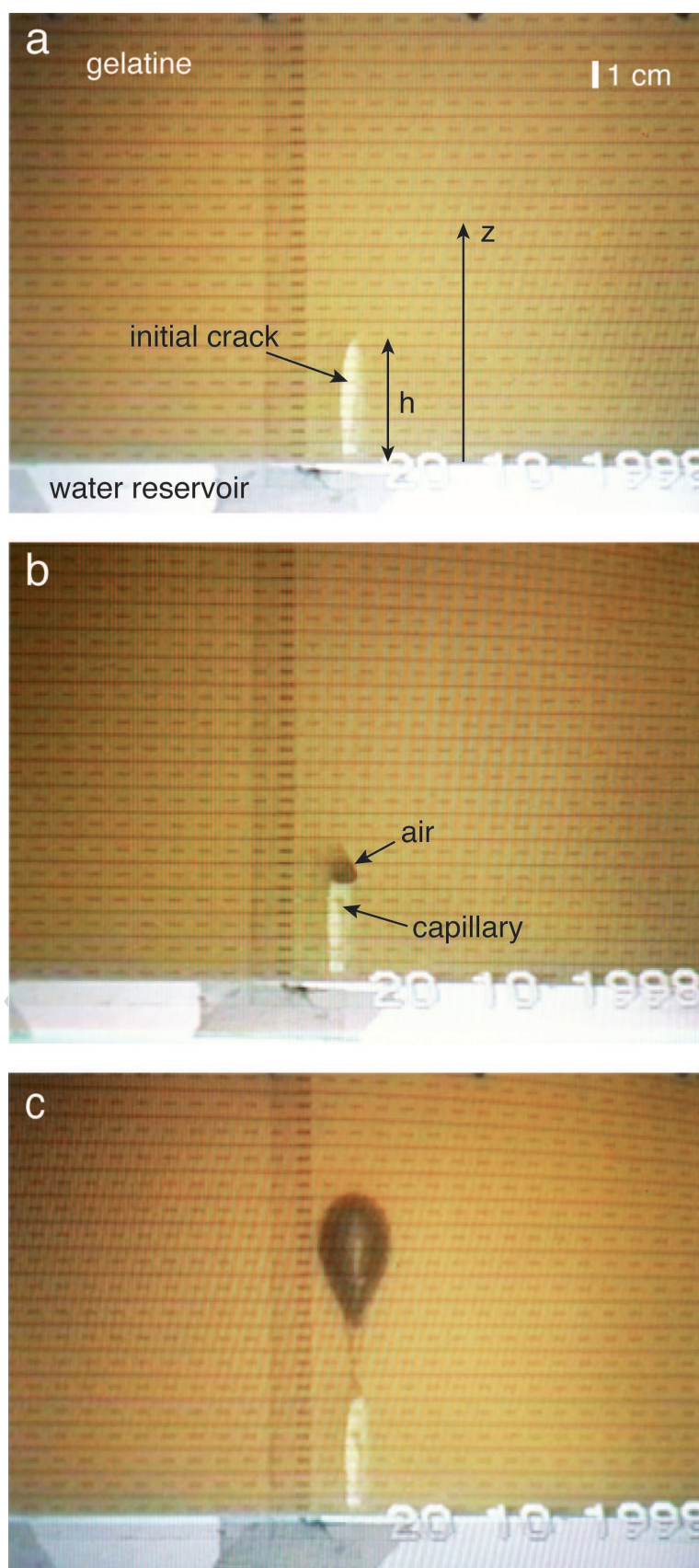


Figure 3

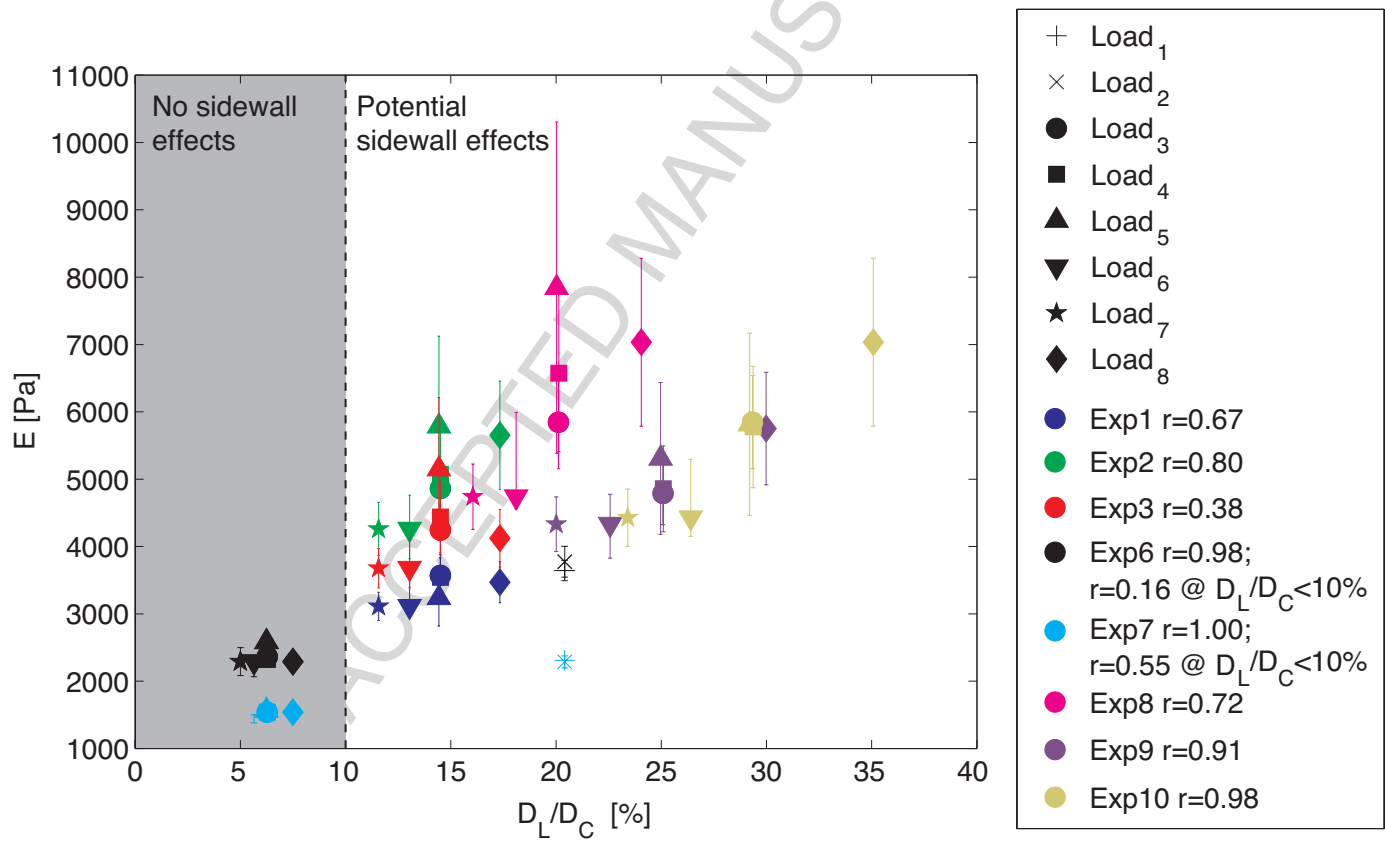


Figure 4

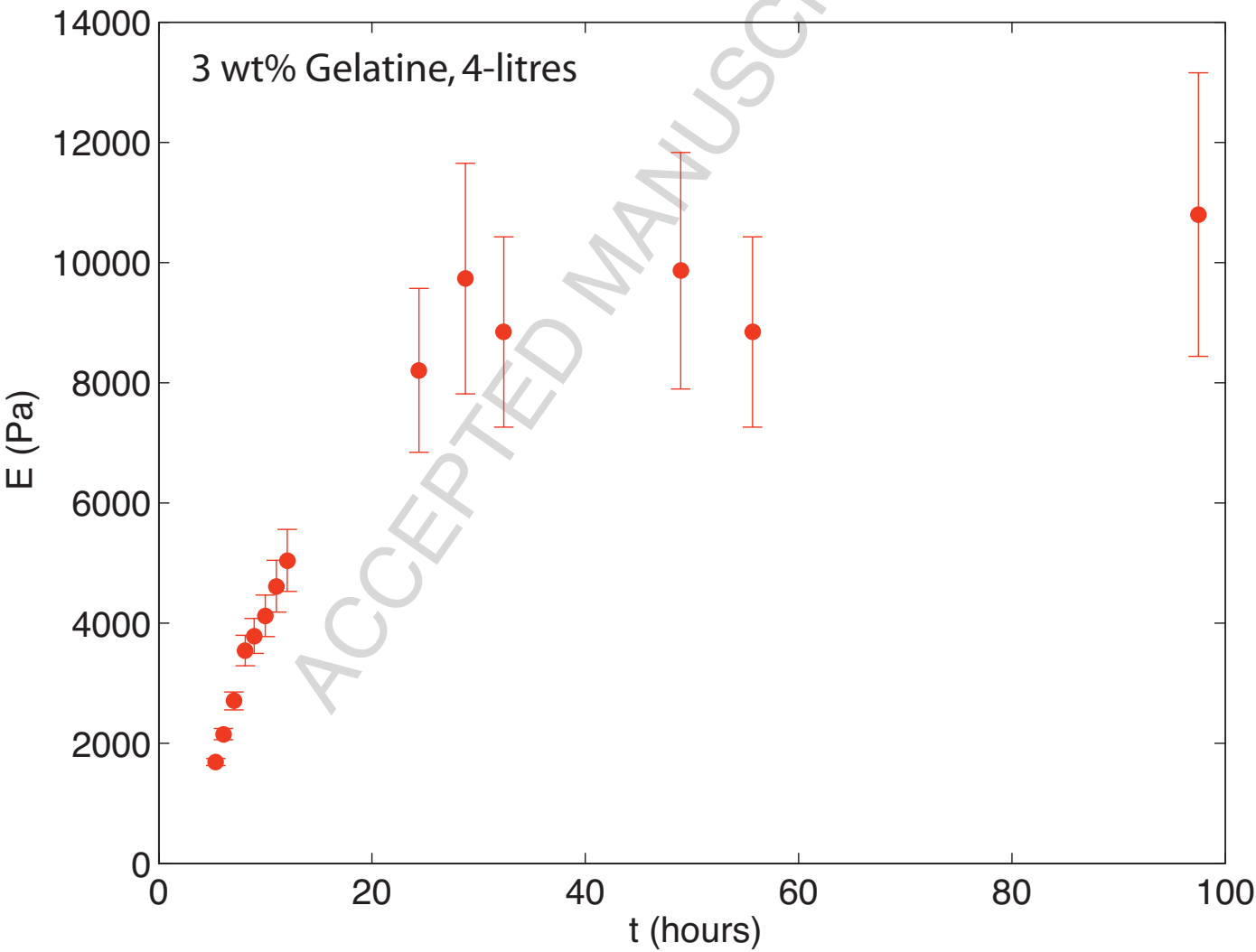


Figure 5

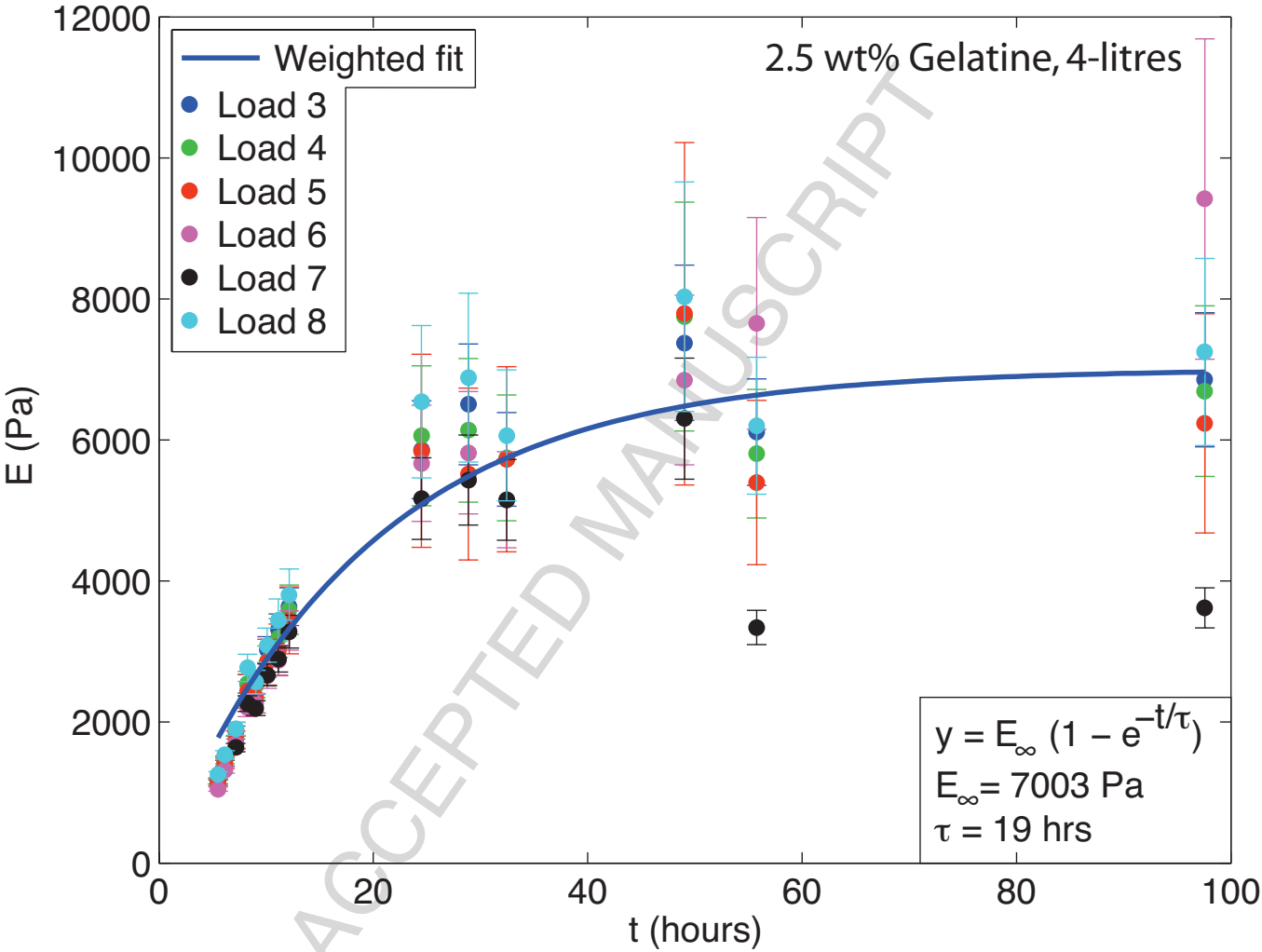


Figure 6

ACCEPTED MANUSCRIPT

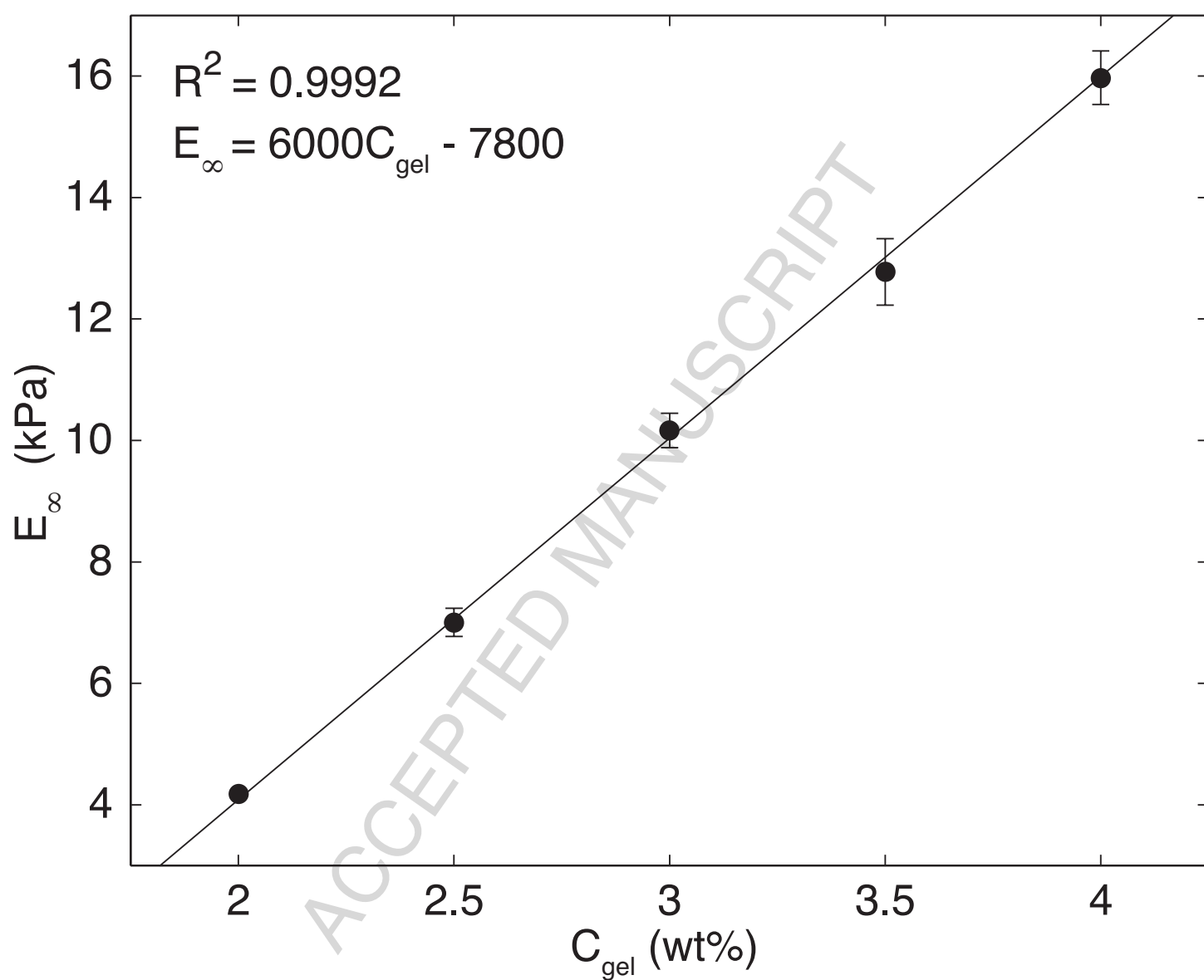


Figure 7

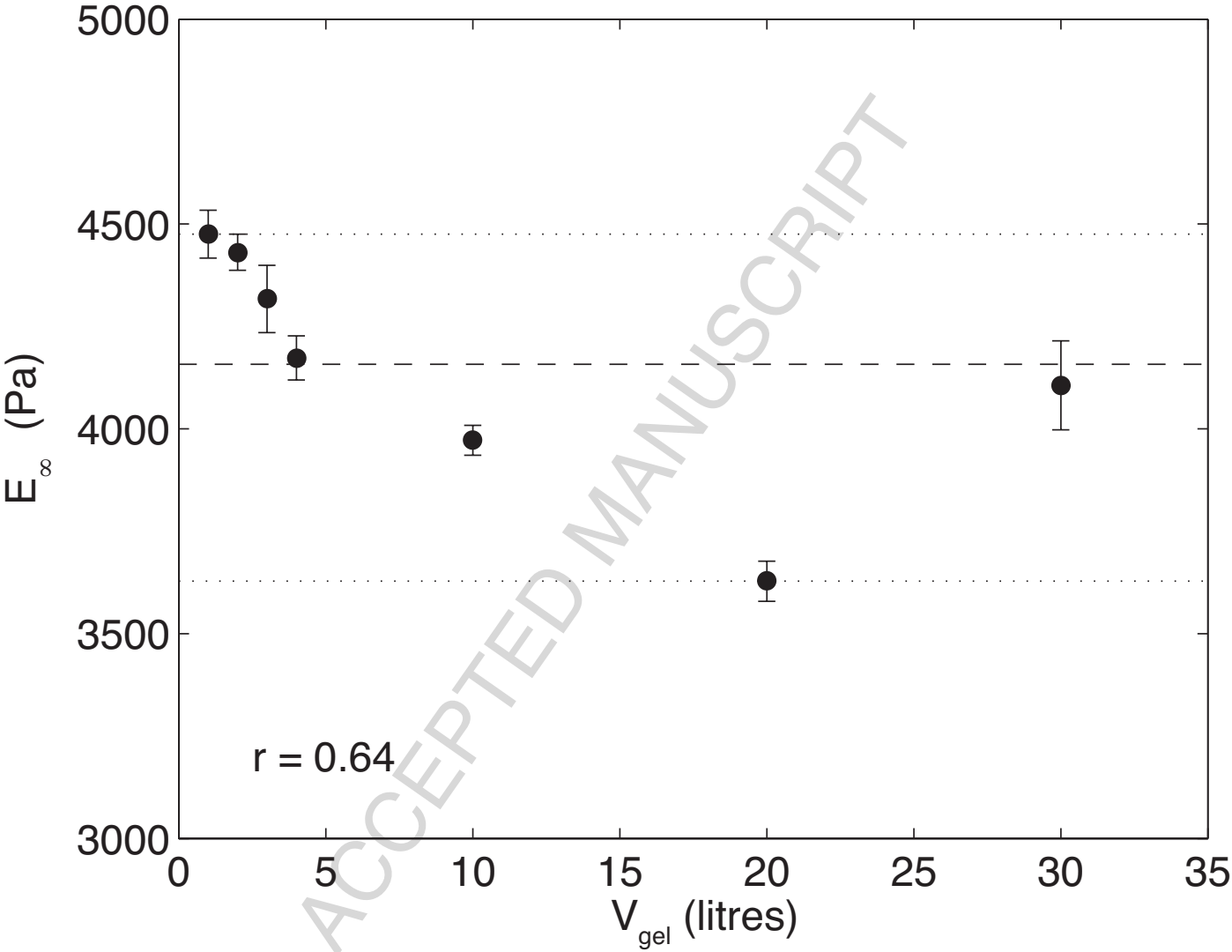


Figure 8

ACCEPTED MANUSCRIPT

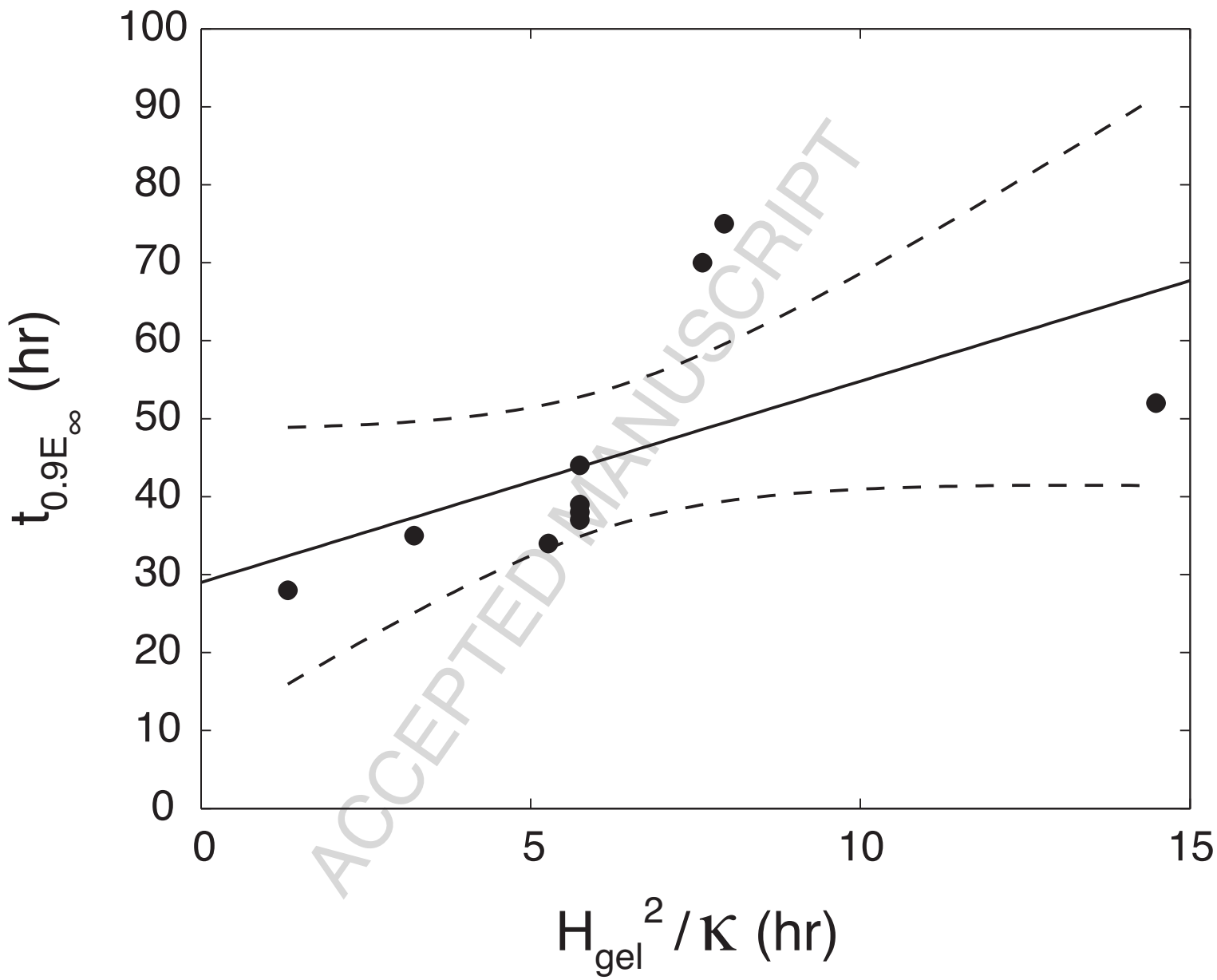




Figure 9

